

Research Article

A Hybrid Smoothed Finite Element Method for Predicting the Sound Field in the Enclosure with High Wave Numbers

Haitao Wang ^{1,2}, Xiangyang Zeng,^{1,2} and Ye Lei^{1,2}

¹School of Marine Science and Technology, Northwestern Polytechnical University, Xi'an 710072, China

²Key Laboratory of Ocean Acoustics and Sensing, Northwestern Polytechnical University, Ministry of Industry and Information Technology, Xi'an, China

Correspondence should be addressed to Haitao Wang; wht@nwpu.edu.cn

Received 19 January 2019; Accepted 15 March 2019; Published 1 April 2019

Academic Editor: Simone Cinquemani

Copyright © 2019 Haitao Wang et al. This is an open access article distributed under the Creative Commons Attribution License, which permits unrestricted use, distribution, and reproduction in any medium, provided the original work is properly cited.

Wave-based methods for acoustic simulations within enclosures suffer the numerical dispersion and then usually have evident dispersion error for problems with high wave numbers. To improve the upper limit of calculating frequency for 3D problems, a hybrid smoothed finite element method (hybrid SFEM) is proposed in this paper. This method employs the smoothing technique to realize the reduction of the numerical dispersion. By constructing a type of mixed smoothing domain, the traditional node-based and face-based smoothing techniques are mixed in the hybrid SFEM to give a more accurate stiffness matrix, which is widely believed to be the ultimate cause for the numerical dispersion error. The numerical examples demonstrate that the hybrid SFEM has better accuracy than the standard FEM and traditional smoothed FEMs under the condition of the same basic elements. Moreover, the hybrid SFEM also has good performance on the computational efficiency. A convergence experiment shows that it costs less time than other comparison methods to achieve the same computational accuracy.

1. Introduction

Small enclosures, such as small studios and aircraft cabins, are typical environments that require high sound quality and low noise level in people's daily life. Prediction on acoustic behavior inside small enclosures using a simulation method has been a basic step in the design of such spaces. The finite element method (FEM) is accepted as an effective numerical strategy for solving low-frequency acoustic field [1]. However, it is well known that the accuracy of the FEM tends to deteriorate with increasing wave number [2, 3]. Many efforts are currently spent on improving performance of the wave-based solution with high wave numbers [4–8].

To obtain precise results in the higher frequency range in FEM, a widely used strategy is reducing the element size and subsequently obtaining fine elements from the model. However, this strategy actually works within the framework of the standard FEM. It does not essentially avoid the problem of precision degradation at midfrequencies and often leads to a heavy computational burden. Therefore,

numerical methods that try to essentially improve the accuracy with high wave numbers based on the mathematical modifications have attracted much attention.

The precision degradation of the standard FEM in midfrequencies is mainly caused by the numerical dispersion [9], which is generated due to the discrete form of the model. In the discrete model, the speed of sound is usually higher than the real one in the continuous medium. It means that the sound wave seems to propagate in some media which are stiffer than the real medium. That is the reason why the standard FEM is usually called an “overly stiff” method. For one-dimensional problems, the studies have demonstrated that the dispersion error can be avoided. While for two- and three-dimensional problems, it has been proven that no methods are dispersion free [10–13].

Among different attempts to reduce the dispersion error, the smoothing technique-based approach that proposed and quickly developed in the past decade shows strong competitiveness from both aspects of computational accuracy and efficiency. The smoothing technique-based

method was originally proposed in the mechanical field. Liu extended the strain smoothing technique in meshless method [14] to the finite element method and named the resulting method the smoothed finite element method (SFEM) [15, 16]. In this method, a set of compatible strain fields named smoothing domains is constructed based on the standard finite element mesh system. Then the stiff matrix in the system equation is reconstructed based on these smoothing domains. By solving the new system equation, the SFEM can achieve better solution at higher frequencies with making very little changes to the standard FEM formulation. Based on the good performances in the mechanical field, the SFEM was naturally introduced into acoustic simulations. Studies have found that it is capable of offering simple and practical ways to weaken the influence of the numerical dispersion. More accurate results can be achieved with high wave numbers by using the smoothing technique. It indicates that the smooth technique can effectively “soften” the overly stiff FEM model.

The smoothing technique in SFEM usually can be performed based on different types of smoothing domains which are created from the nodes, edges, cells, or faces of the elements. Therefore, the SFEM can be generally categorized into the following types, the node-based smoothed finite element method (NS-FEM) [17], the edge-based smoothed finite element method (ES-FEM) [18–21], the cell-based smoothed finite element method (CS-FEM) [22, 23], and the face-based smoothed finite element method (FS-FEM) [24–26]. Among these SFEMs, the NS-FEM possesses a special property that the stiff matrix obtained by NS-FEM is “softer” than the exact one. In such a condition, upper bound solution can be obtained with respect to the exact solution. However, the NS-FEM makes the stiffness matrix “overly soft,” which leads that the NS-FEM does not show evident advantage on the computational accuracy. On the contrary, other SFEMs show opposite properties for 3D acoustic problems. They provide softer stiff matrices than the standard FEM, but the stiffness matrices are still overestimated than the exact one. Therefore, lower bound solutions can be obtained with respect to the exact solution by using these SFEMs.

To further improve the performance of the smoothed methods, the α -FEM [27–30] was proposed by mixing the node-based technique and the standard FEM. Due to the fact that the NS-FEM has opposite properties on the stiffness with respect to the standard FEM, the α -FEM can obtain good features from both techniques and therefore give closer stiffness to the exact one once the smoothing domains are properly constructed. More recently, the theory of mixed smoothed methods was further developed and the β -FEM [31, 32], which mixes the node-based technique and the edge-based technique, was proposed and used for solving the mechanical problems. Since the smoothed techniques usually have better accuracy than the standard FEM, the β -FEM including the combination of both smoothing techniques has potential to achieve better accuracy than the α -FEM.

Inspired by the idea of β -FEM, a hybrid smoothed finite element method (hybrid SFEM) for solving 3D acoustical problems is proposed in this paper. The essential idea of the hybrid SFEM is to construct a stiffness model by mixing the

node-based and face-based techniques. Based on the truth that the number of faces in a tetrahedron element is always less than that of the edges, the face-based smoothing domains are much easier to be constructed than the edge-based smoothing domains. Therefore, the proposed hybrid SFEM has high efficiency on constructing the mixed smoothing domains. The numerical verifications have demonstrated that the proposed method is capable of significantly reducing the numerical dispersion and giving more accurate results.

2. Hybrid SFEM for Acoustic Simulation in Enclosure

2.1. Acoustic Simulation in Enclosure. Consider a steady-state acoustic problem in an enclosure. A closed boundary surrounds a bounded fluid domain V , which is characterized by its speed of sound c and its ambient fluid density ρ_0 . The fluid domain is excited at a circular frequency ω by using an acoustic point source with prescribed volume velocity q located at position $r_q = [x_q, y_q, z_q]^T$. Assuming that the system is linear, the fluid is inviscid, and the process is adiabatic, the steady-state acoustic pressure p in the problem domain is governed by using the Helmholtz equation:

$$\nabla^2 p + k^2 p + j\rho_0\omega q = 0, \quad (1)$$

where ∇^2 is the Laplacian operator, k denotes the wave number and is defined by ω/c , and j is the imaginary unit.

By using the weighted residual method and applying the boundary condition, the integral equation to calculate the sound pressure can be obtained as follows:

$$\int_{\Omega} (\nabla p \cdot \nabla p - k^2 p \cdot p - j\rho_0\omega p q_w) d\Omega + \int_{\Gamma} j\rho_0\omega \frac{p}{Z} \cdot p d\Gamma = 0, \quad (2)$$

where Ω and Γ represent the problem domain and the boundary domain, respectively. Z is the specific acoustic impedance of the boundary.

By dividing the problem domain into discretizing form, the sound pressure at any position in the problem domain can be expressed by

$$p = \sum_{i=1}^n N_i p_i = \mathbf{N}^T \mathbf{p}, \quad (3)$$

where n is the number of nodes, \mathbf{N} is the vector of the shape functions, and \mathbf{p} is the vector of nodal sound pressures yet to be determined.

By substituting equation (3) into equation (2), the system equation to solve the discretizing nodal pressure can be finally obtained as follows:

$$(\mathbf{K} + j\omega\mathbf{C} - \omega^2\mathbf{M})\mathbf{p} = \mathbf{F}, \quad (4)$$

where $\mathbf{K} = \int_{\Omega} (\nabla\mathbf{N})(\nabla\mathbf{N})^T d\Omega$ is defined as the stiffness matrix, $\mathbf{M} = (1/c^2) \int_{\Omega} \mathbf{N}\mathbf{N}^T d\Omega$ is defined as the mass matrix, $\mathbf{C} = (\rho_0/Z) \int_{\Gamma} \mathbf{N}\mathbf{N}^T d\Gamma$ is defined as the damping matrix, and $\mathbf{F} = \int_{\Omega} j\rho_0\omega \mathbf{N} q_w d\Omega$ is the load vector.

2.2. Briefing of NS-FEM and FS-FEM. It has been mentioned that the standard FEM usually behaves overly stiff in the

calculation. To soften the stiffness of the FEM model by using the smoothing technique, a set of smoothing domains needs to be constructed based on the basic elements first. Assuming the fluid domain inside a 3D cavity has been divided into tetrahedral elements, the smoothing domains of the NS-FEM and FS-FEM based on these basic elements are illustrated in Figure 1.

The smoothing domains for NS-FEM are generated based on the nodes of the elements such that $\Omega_{\text{NS}} = \cup_{m=1}^{N_n} \Omega_m^{\text{NS}}$ and $\Omega_i^{\text{NS}} \cap \Omega_j^{\text{NS}} = \emptyset$ for $i \neq j$. Here N_n is the total number of nodes in the problem domain, Ω_m^{NS} is the smoothing domain associated with the node m . Moreover, when there are two or more elements sharing the node m , Ω_m^{NS} can be formed by using $\Omega_m^{\text{NS}} = \cup_{t=1}^{N_{m,e}} \Omega_{m,t}^{\text{NS}}$, where $N_{m,e}$ is the number of elements that share node m . As illustrated in Figure 1(a), in the condition of tetrahedron element, $\Omega_{m,t}^{\text{NS}}$ is formed by connecting the node m , three central points of the edges, and the centroid of the element. According to this method to construct the smoothing domain, all the subsmoothing domains are nonoverlapping each other and also without gaps to fill the whole problem domain.

In NS-FEM formulation, the gradient smoothing operation is applied over each smoothing domain on the gradient of acoustic pressure ∇p , and the smoothed gradient of acoustic pressure for Ω_m^{NS} can be written as

$$\overline{\nabla p}(\Omega_m^{\text{NS}}) = \frac{1}{V_m} \int_{\Omega_m^{\text{NS}}} \nabla p d\Omega, \quad (5)$$

where V_m is the volume of the smoothing domain Ω_m^{NS} .

By applying the divergence theorem, the smoothed gradient of acoustic pressure can be expressed in terms of acoustic pressure:

$$\overline{\nabla p}(\Omega_m^{\text{NS}}) = \frac{1}{V_m} \int_{\Gamma_m} p \cdot \mathbf{n} d\Gamma, \quad (6)$$

where Γ_m denotes the boundary of the smoothing domain Ω_m^{NS} and \mathbf{n} is the vector of the components of the outward normal vector to the boundary Γ_m and is expressed by $\mathbf{n} = [n_x, n_y, n_z]^T$.

By using the FEM shape function for field variable interpolation in the form of equation (3), the acoustic pressure at a position x on the boundary of the smoothing domain is calculated by

$$p(x) = \sum_{I \in D_m} N_I(x) p_I, \quad (7)$$

where D_m is a set of the so-called supporting nodes of node m , which is a group of nodes belonging to the elements that shares the node m . $N_I(x)$ is the shape function of node I , and p_I is the nodal acoustic pressure.

By substituting equation (7) into equation (6), the smoothed gradient of pressure can be written as follows:

$$\begin{aligned} \overline{\nabla p}(\Omega_m^{\text{NS}}) &= \frac{1}{V_m} \int_{\Gamma_m} \left(\sum_{I \in D_m} N_I(\mathbf{x}) p_I \right) \cdot \mathbf{n}(\mathbf{x}) d\Gamma \\ &= \sum_{I \in D_m} \mathbf{B}_{mI}^{\text{NS}} p_I = \widehat{\mathbf{B}}_m^{\text{NS}} \mathbf{P}, \end{aligned} \quad (8)$$

where $\widehat{\mathbf{B}}_m^{\text{NS}} = [\mathbf{B}_{m1}^{\text{NS}}, \mathbf{B}_{m2}^{\text{NS}}, \dots, \mathbf{B}_{mj}^{\text{NS}}]$ is vector of the so-called smoothed derivative of the shape function and J denotes the number of nodes in the set D_m . The I th element of $\widehat{\mathbf{B}}_m^{\text{NS}}$ can be calculated by the following form:

$$\mathbf{B}_{mI}^{\text{NS}} = \frac{1}{V_m} \int_{\Gamma_m} N_I(\mathbf{x}) \cdot \mathbf{n}(\mathbf{x}) d\Gamma. \quad (9)$$

By replacing ∇p in equation (2) with $\overline{\nabla p}$, the local smoothed stiffness matrix for the smoothing domain Ω_m^{NS} can be obtained:

$$\mathbf{K}_m^{\text{NS}} = \int_{\Omega_m} \left(\widehat{\mathbf{B}}_m^{\text{NS}} \right)^T \widehat{\mathbf{B}}_m^{\text{NS}} d\Omega = \left(\widehat{\mathbf{B}}_m^{\text{NS}} \right)^T \widehat{\mathbf{B}}_m^{\text{NS}} V_m. \quad (10)$$

Then, the global smoothed stiffness matrix can be assembled by the local smoothed stiffness matrix over each smoothing domains as

$$\mathbf{K}^{\text{NS}} = \sum_{m=1}^{N_n} \mathbf{K}_m^{\text{NS}}. \quad (11)$$

Similar to the NS-FEM, the FS-FEM also requires that the problem domain is divided into smoothing domains, while these smoothing domains are constructed based on the faces of the basic elements such that $\Omega_{\text{FS}} = \cup_{m=1}^{N_f} \Omega_m^{\text{FS}}$ and $\Omega_i^{\text{FS}} \cap \Omega_j^{\text{FS}} = \emptyset$ for $i \neq j$. When there are two elements sharing the face m , Ω_m^{FS} can be formed by $\Omega_m^{\text{FS}} = \cup_{t=1}^2 \Omega_{m,t}^{\text{FS}}$. As illustrated in Figure 1(b), in the condition of tetrahedron element, $\Omega_{m,t}^{\text{FS}}$ is formed by connecting the three nodes of the face m and the centroid of the element. Based on the same derivation, the global smoothed stiffness matrix for FS-FEM can be derived as

$$\mathbf{K}^{\text{FS}} = \sum_{m=1}^{N_f} \mathbf{K}_m^{\text{FS}}, \quad (12)$$

where N_f is the total number of the faces of the basic elements. \mathbf{K}_m^{FS} is the local smoothed stiffness matrix for the smoothing domain Ω_m^{FS} .

2.3. Hybrid SFEM. Considering the overestimation property of FS-FEM and the unique underestimation property of NS-FEM, the smoothing domains for the hybrid method are constructed as illustrated in Figure 2.

In this paper, the strategy for constructing the smoothing domain is developed based on the tetrahedron element which is a type of element that can be used to simply discrete the complicated-shaped spaces. As illustrated in Figure 2, a single element is divided into two types of smoothing domains, namely, the node-based and the face-based smoothing domains. Each edge of the element is truncated by two points which locate on the 1/4 positions of the edge, which can be expressed by the relation that $l_1 = 2l_2$. After the smoothing domains are formed in each element, the local smoothing domains can be subsequently constructed by combining the ones in neighboring elements as mentioned in the last subsection.

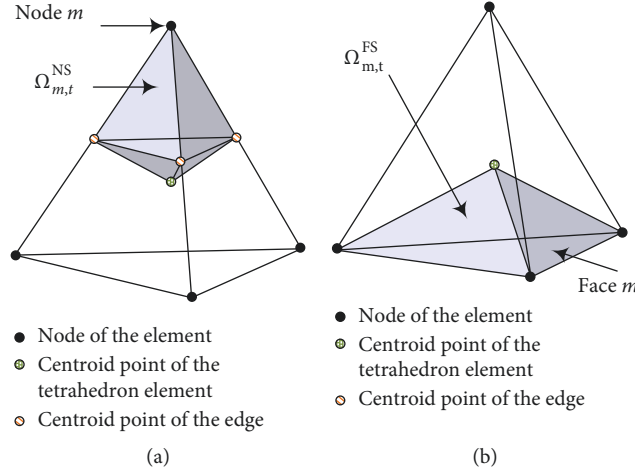


FIGURE 1: Node-based and (a) face-based (b) smoothing domains constructed based on the tetrahedron element.

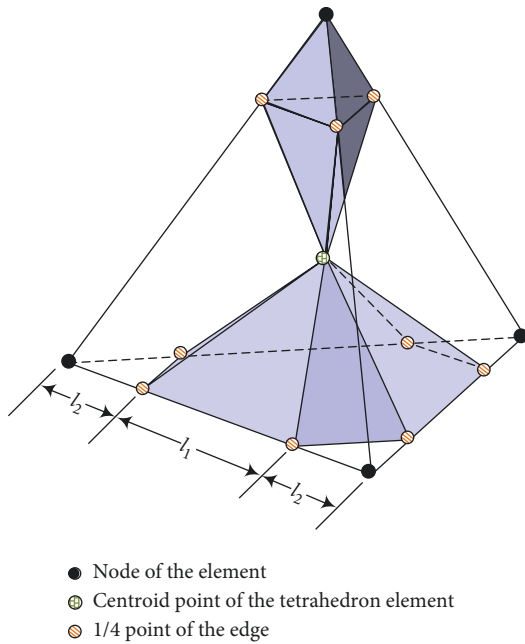


FIGURE 2: Mixed smoothing domain constructed based on the tetrahedron elements.

Based on the hybrid node-based and face-based smoothing domains, the global hybrid smoothed stiffness matrix can be obtained by

$$\bar{\mathbf{K}} = \mathbf{K}^{\text{NS}} + \mathbf{K}^{\text{FS}} = \sum_{m=1}^{N_n} \mathbf{K}_m^{\text{NS}} + \sum_{m=1}^{N_f} \mathbf{K}_m^{\text{FS}}. \quad (13)$$

This equation demonstrates that the smoothed stiffness matrix is constructed using the shape functions but not the derivatives of the shape functions. This implies that the requirement on the nodal shape function is further weakened compared to the standard FEM [33, 34]. By replacing the stiffness matrix in equation (4) with the smoothed stiffness matrix, the hybrid SFEM is formulated and can be used to calculate the sound field in an enclosure.

3. Numerical Verification

This section discusses the results of a numerical verification performed on a convex 3D cubic cavity as shown in Figure 3(a). The interior of the cavity with dimensions $1 \times 1.2 \times 1.4$ m is filled with air characterized by speed of sound $c = 344$ m/s and density $\rho_0 = 1.21$ kg/m³. There is a sound source and a receiver located inside the cavity, and their locations are (0.1, 0.1, 0.1) m and (0.74, 0.71, 0.93) m, respectively.

For the standard FEM, the cavity is divided into 384 tetrahedron elements as shown in Figure 3(b). These elements are also used as the basic elements for NS-FEM, FS-FEM, and the proposed hybrid SFEM. The impedance of the inner surfaces is set to be $400\rho_0c$.

To evaluate the performance of the proposed method on reducing the numerical dispersion, the modal frequencies are firstly calculated using the proposed method and compared with those obtained using the standard FEM, NS-FEM, and FS-FEM. The modal frequencies are also calculated using the normal-mode theory and used as the standard reference result. The comparisons and relative errors are illustrated in Figure 4.

Figure 4(a) illustrates that all methods are capable of giving the same results with the reference results at low mode orders. With the increase of the mode order, the results of the wave-based methods begin to deviate from those of the normal-mode theory. It is evident that larger mode order will cause larger deviation of the results, which means the accuracy degradation of the wave-based methods become larger with increasing the wave number. It can also be found that the results of NS-FEM are always smaller than the reference results, while other methods give larger results. It demonstrates that NS-FEM has a special property that it is “overly soft” to simulate the acoustic field. By considering the normal-mode theory as the reference method, the relative errors in Figure 4(b) show that the proposed hybrid SFEM has better accuracy than other methods. It gives the same results with the reference method at low mode orders. Moreover, its

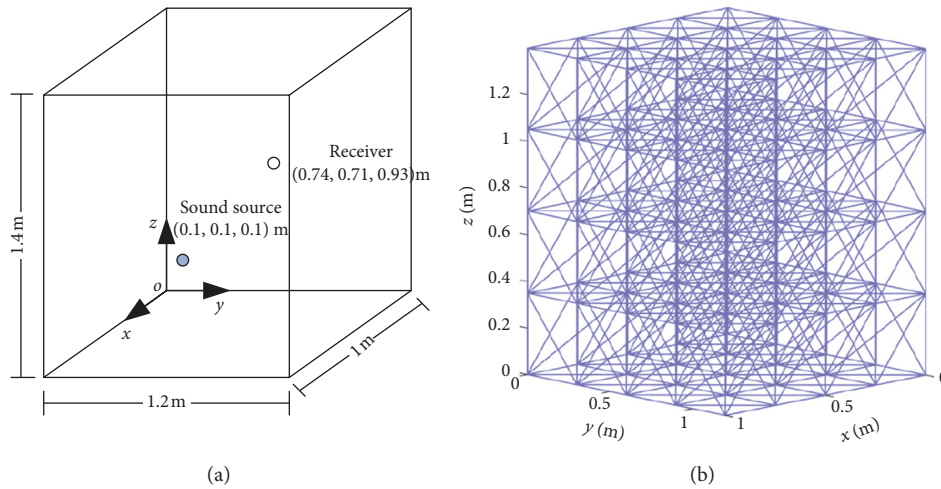


FIGURE 3: Schematics of the 3D cubic cavity and its discrete form. (a) The cubic cavity and its dimensions. (b) The tetrahedron elements of the fluid domain.

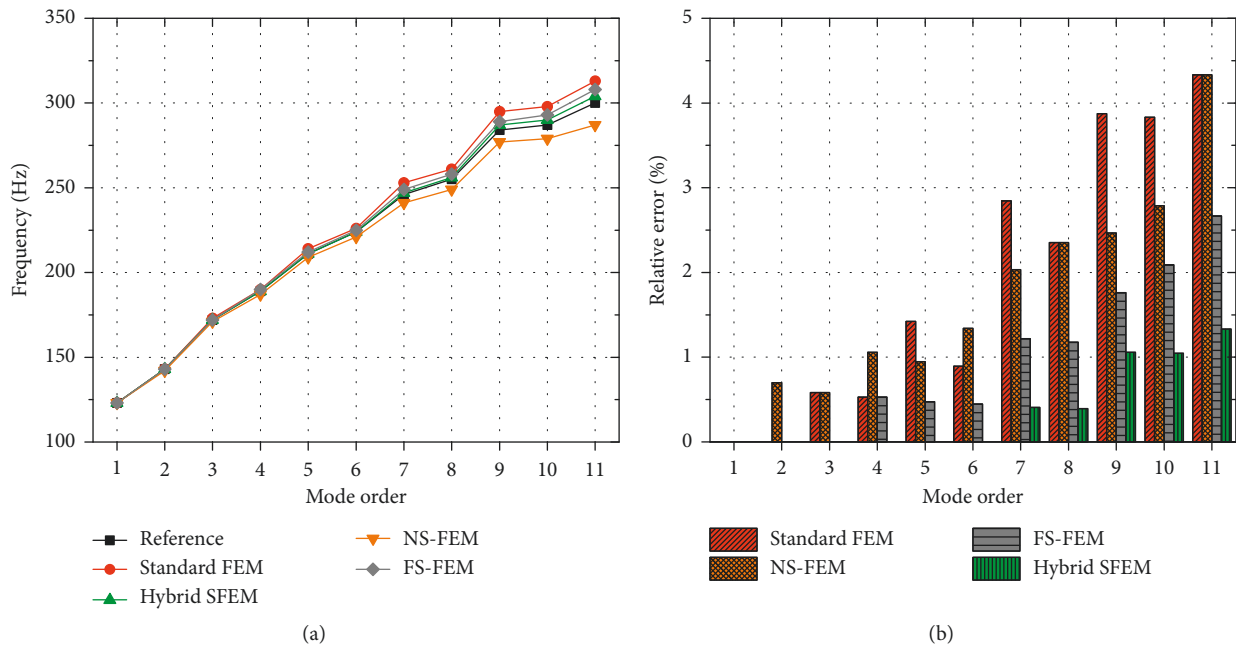


FIGURE 4: (a) The first 11 modal frequencies obtained by the reference method, standard FEM, hybrid SFEM, NS-FEM, and FS-FEM. (b) The relative errors of the standard FEM, hybrid SFEM, NS-FEM and FS-FEM.

relative errors are basically smaller than 2%, while other methods have evident larger errors.

The calculations on the modal frequencies have preliminarily proved that the proposed hybrid SFEM has better accuracy than other wave-based methods. To give a further verification, the distributions of sound pressure level at the top surface of the cavity are also compared as illustrated in Figure 5. The acoustic velocity vectors are also illustrated in Figure 6.

According to the aforementioned element setup of this problem, the average nodal spacing is about 0.33 m, which gives a frequency limit of about 171 Hz by “the rule of thumb.” To investigate the performance of the proposed

method, the results at 270 Hz are compared here. Note that since Figure 4(b) has demonstrated that the standard FEM has the largest errors and it is no longer included in the comparisons in the following verifications.

Figure 5(c) illustrates that the NS-FEM solution shows obvious dispersion error, as most of the contours of the sound pressure level are departing from the reference solution. Both the FS-FEM and hybrid SFEM can provide similar contours to the reference, while the Hybrid SFEM has better accordance with the reference than the FS-FEM at the corner positions. The acoustic velocity vectors shown in Figure 6 also illustrate the effectiveness of the proposed method. Figure 6(b) show that the vectors have very similar

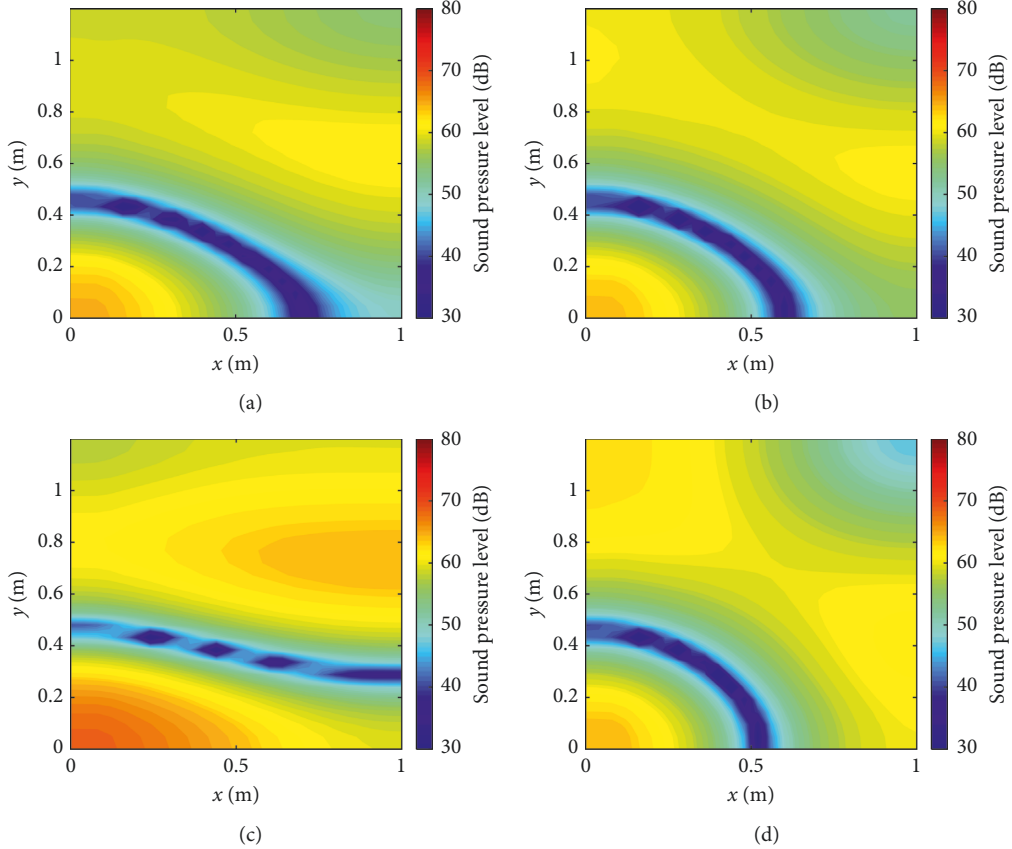


FIGURE 5: Distributions of sound pressure level at the top surface of the cavity at 270 Hz. (a) Reference method. (b) Hybrid SFEM. (c) NS-FEM. (d) FS-FEM.

directions and lengths with the reference results, while other methods have larger differences.

At last, the frequency responses at the receiver are calculated using different methods and illustrated in Figure 7. It shows that all the wave-based methods have satisfactory accuracies when the frequency is less than 175 Hz. However, the accuracies of all the methods tend to deteriorate by increasing the calculating frequency. It can be seen that the NS-FEM starts to have dispersion error at about 185 Hz, which demonstrates that the NS-FEM has worse performance on weakening the numerical dispersion than other methods based on the same basic elements. Moreover, the modal frequencies obtained by the NS-FEM are less than the exact ones. It proves that the NS-FEM holds the characteristic of behaving “softly” compared with the exact stiffness. Then, it can be seen that the proposed hybrid SFEM and the FS-FEM start to have dispersion error at about 250 Hz. By analyzing the differences of the modal frequencies, it can be found that the hybrid SFEM has less dispersion error than the FS-FEM. The comparisons in this figure demonstrates that the hybrid SFEM can give more precise results than the other two methods based on the same basic elements.

The calculating efficiency is another basic index to evaluate the performance of a wave-based method. According to the basic theory of the proposed method, it can be known that the differences of the methods on the

computational time are mainly caused by different constructing methods of the stiffness matrices. To clearly illustrate the relations between the computational time and accuracy of different methods, the modal frequency which is only related to the stiffness matrix and the mass matrix is chosen as the analysis parameter and a convergence analysis is performed and shown in Figure 8. In this numerical experiment, the former 20 orders of the modal frequencies of the aforementioned cubic cavity are calculated by the standard FEM, NS-FEM, FS-FEM, and the hybrid SFEM. Based on these results, the average relative errors defined by the following equation are calculated:

$$\varepsilon = \frac{1}{20} \sum_{m=1}^{20} \left| \frac{f_m - \tilde{f}_m}{\tilde{f}_m} \right| \times 100\%, \quad (14)$$

where f_m and \tilde{f}_m denote the m th order of the modal frequency calculated by the wave-based method and reference method, respectively.

The average relative errors of different methods are all obtained under 4 different meshing densities, for which the number of the basic tetrahedron elements is 162, 384, 750, and 1296, respectively. All the calculations are performed under the configuration of Inter® Core™ i3-4150CPU @3.50 GHz, 16 GB RAM.

It is well known that the computational efficiency of the wave-based method is closely related with the number of

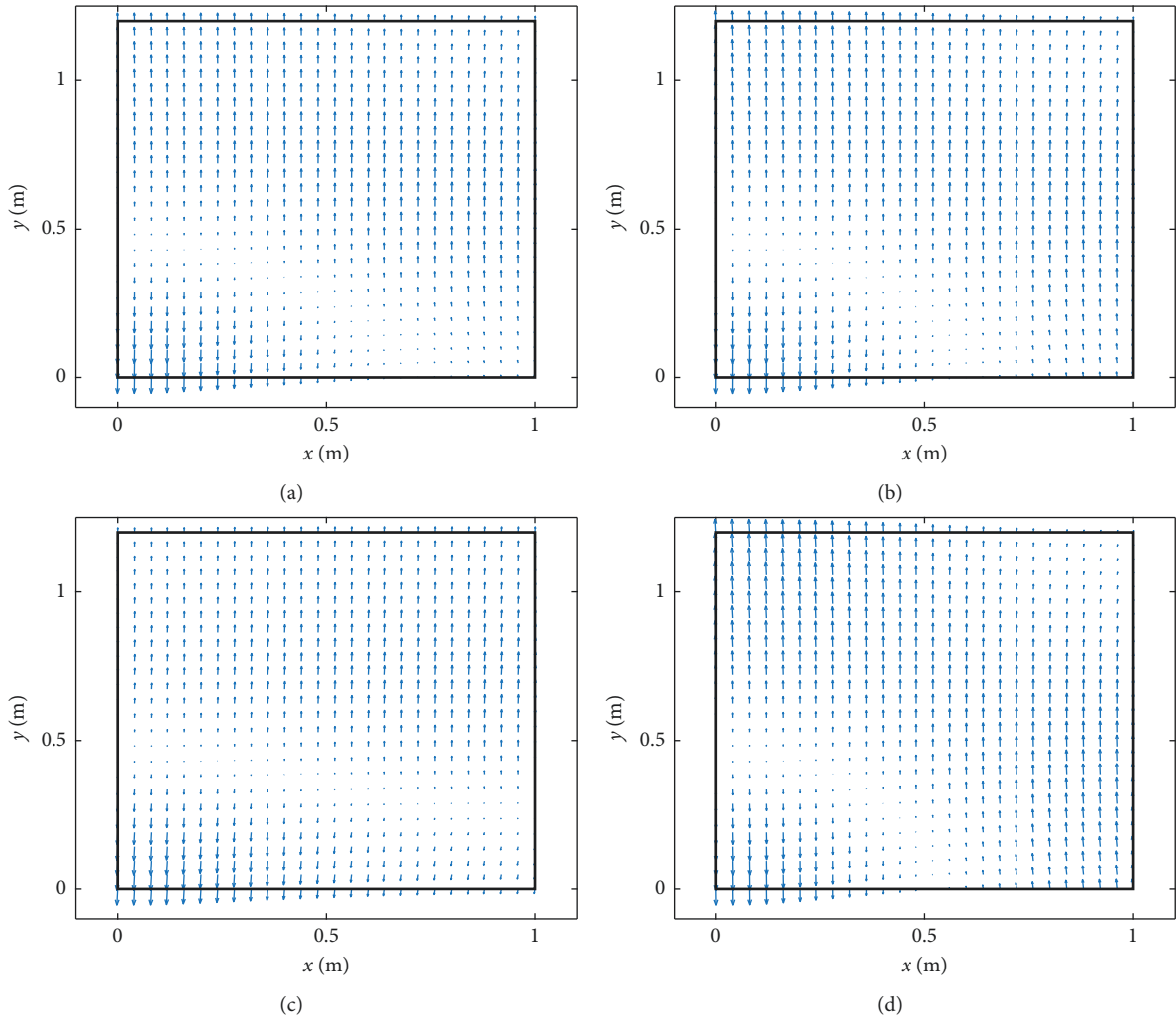


FIGURE 6: Acoustic velocity vectors at the top surface of the cavity at 270 Hz. (a) Reference method. (b) Hybrid SFEM. (c) NS-FEM. (d) FS-FEM.

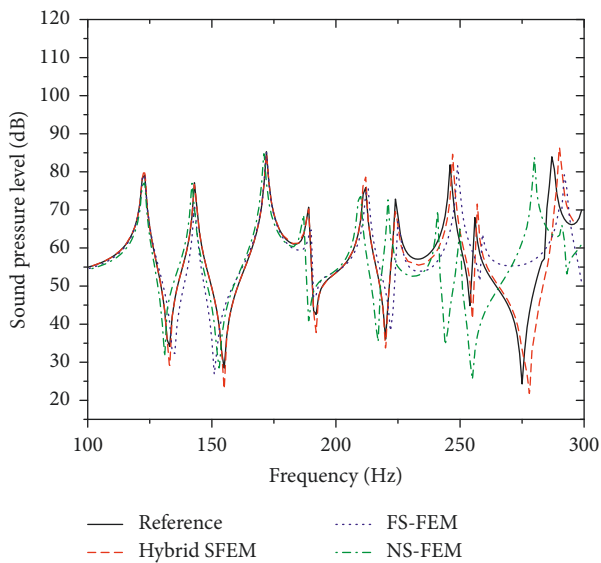


FIGURE 7: Frequency responses of different methods from 100 Hz to 300 Hz.

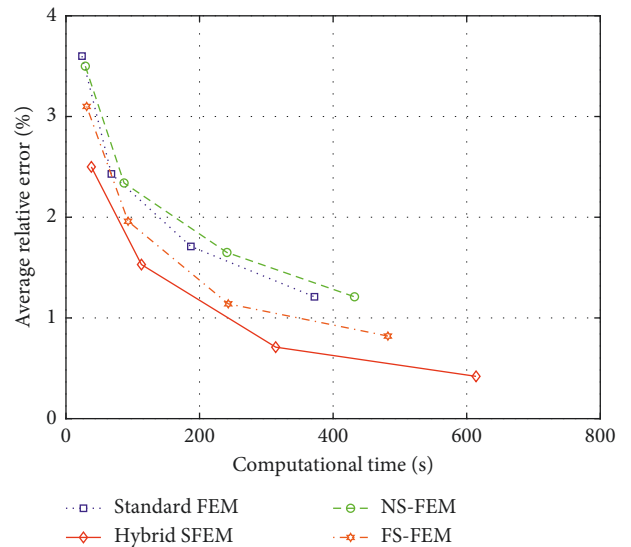


FIGURE 8: Convergence curves for different methods.

elements in the calculation. In this case, if the calculations are performed based on the same basic elements, it is evident that the standard FEM will cost least time to complete the calculations, while the smoothed methods will cost more time, and the hybrid SFEM will cost the most time. This is because that, in the smoothed finite elements methods, the construction of the stiffness matrix is performed based on the smoothing domains of which the number is usually larger than the basic element. However, the conclusion will be much more different if the efficiency is analyzed from a convergence aspect of view. Figure 8 shows that the hybrid SFEM can achieve the highest accuracy in terms of the same computational time among different methods. Meanwhile, the hybrid SFEM costs least time to obtain the results that have the same average relative errors with other methods.

4. Conclusion

In this work, a hybrid SFEM is proposed and applied for 3D acoustic simulation in a small enclosure. In this method, the traditional node-based and face-based smoothed finite element methods are mixed to form a new smoothed model through constructing the mixed smoothing domains. According to the smoothed theory, the exact solution is bounded by the results of the NS-FEM and FS-FEM. Therefore, the hybrid SFEM is promising to achieve better accuracy by obtaining the contributions from both smoothed methods. Through the formulation and numerical verifications, the results show that the hybrid SFEM has better accuracy than the standard FEM, NS-FEM, and FS-FEM based on the same basic elements. The verifications demonstrate that the hybrid SFEM is effective to reduce the numerical dispersion and improve the upper limit of the calculating frequency.

Data Availability

The data that support the findings of this study are available from the corresponding author via e-mail (wht@nwpu.edu.cn) upon reasonable request.

Conflicts of Interest

The authors declare that there are no conflicts of interest regarding the publication of this paper.

Acknowledgments

The author wish to thank the National Natural Science Foundation of China (grant no. 11604266) and the Fundamental Research Funds for the Central Universities (grant nos. 3102017gx06009 and MJ-2015-F-044) for their financial support.

References

- [1] L. L. Thompson, "A review of finite-element methods for time-harmonic acoustics," *Journal of the Acoustical Society of America*, vol. 119, no. 3, pp. 1315–1330, 2006.
- [2] F. Ihlenburg and I. Babuška, "Finite element solution of the Helmholtz equation with high wave number part I: the h-version of the FEM," *Computers & Mathematics with Applications*, vol. 30, no. 9, pp. 9–37, 1995.
- [3] F. Ihlenburg and I. Babuška, "Finite element solution of the Helmholtz equation with high wave number part II: the h-p version of the FEM," *SIAM Journal on Numerical Analysis*, vol. 34, no. 1, pp. 351–358, 1997.
- [4] B. Yue and M. N. Guddati, "Dispersion-reducing finite elements for transient acoustics," *Journal of the Acoustical Society of America*, vol. 118, no. 4, pp. 2132–2141, 2005.
- [5] B. V. Genechten, O. Atak, B. Bergen et al., "An efficient wave-based method for solving Helmholtz problems in three-dimensional bounded domains," *Engineering Analysis with Boundary Elements*, vol. 36, no. 1, pp. 63–75, 2012.
- [6] K. Christodoulou, O. Laghrouche, M. S. Mohamed, and J. Trevelyan, "High-order finite elements for the solution of Helmholtz problems," *Computers & Structures*, vol. 191, pp. 129–139, 2017.
- [7] H. Wu, W. Ye, and W. Jiang, "Isogeometric finite element analysis of interior acoustic problems," *Applied Acoustics*, vol. 100, pp. 63–73, 2015.
- [8] P. Bouillard and S. Suleau, "Element-free Galerkin solutions for Helmholtz problems: formulation and numerical assessment of the pollution effect," *Computer Methods in Applied Mechanics and Engineering*, vol. 162, no. 1–4, pp. 317–335, 1998.
- [9] S. Irimie and P. Bouillard, "A residual a posteriori error estimator for the finite element solution of the Helmholtz equation," *Computer Methods in Applied Mechanics and Engineering*, vol. 190, no. 31, pp. 4027–4042, 2001.
- [10] I. Babuška, F. Ihlenburg, E. T. Paik, and S. A. Sauter, "A generalized finite element method for solving the Helmholtz equation in two dimensions with minimal pollution," *Computer Methods in Applied Mechanics and Engineering*, vol. 128, no. 3–4, pp. 325–359, 1995.
- [11] P. Bouillard and F. Ihlenburg, "Error estimation and adaptivity for the finite element method in acoustics: 2D and 3D applications," *Computer Methods in Applied Mechanics and Engineering*, vol. 176, no. 1–4, pp. 147–163, 1999.
- [12] A. Deraemaeker, I. Babuška, and P. Bouillard, "Dispersion and pollution of the FEM solution for the Helmholtz equation in one, two and three dimensions," *International Journal for Numerical Methods in Engineering*, vol. 46, no. 4, pp. 471–499, 1999.
- [13] I. M. Babuska and S. A. Sauter, "Is the pollution effect of the FEM avoidable for the Helmholtz equation considering high wave numbers?," *SIAM Review*, vol. 42, no. 3, pp. 451–484, 2000.
- [14] J.-S. Chen, C.-T. Wu, S. Yoon, and Y. You, "A stabilized conforming nodal integration for Galerkin mesh-free methods," *International Journal for Numerical Methods in Engineering*, vol. 50, no. 2, pp. 435–466, 2001.
- [15] G. R. Liu, T. T. Nguyen, K. Y. Dai, and K. Y. Lam, "Theoretical aspects of the smoothed finite element method (SFEM)," *International Journal for Numerical Methods in Engineering*, vol. 71, no. 8, pp. 902–930, 2007.
- [16] G. R. Liu, "A Generalized gradient smoothing technique and the smoothed bilinear form for Galerkin formulation of a wide class of computational methods," *International Journal of Computational Methods*, vol. 5, no. 2, pp. 199–236, 2008.
- [17] G. R. Liu, T. Nguyen-Thoi, H. Nguyen-Xuan, and K. Y. Lam, "A node-based smoothed finite element method (NS-FEM) for upper bound solutions to solid mechanics problems," *Computers & Structures*, vol. 87, no. 1–2, pp. 14–26, 2009.
- [18] X. Y. Cui, G. R. Liu, G. Y. Li, G. Y. Zhang, and G. Zheng, "Analysis of plates and shells using an edge-based smoothed

- finite element method,” *Computational Mechanics*, vol. 45, no. 2-3, pp. 141–156, 2010.
- [19] Z. C. He, G. R. Liu, Z. H. Zhong, G. Y. Zhang, and A. G. Cheng, “Coupled analysis of 3D structural-acoustic problems using the edge-based smoothed finite element method/finite element method,” *Finite Elements in Analysis and Design*, vol. 46, no. 12, pp. 1114–1121, 2010.
- [20] Z. C. He, G. Y. Li, Z. H. Zhong et al., “An ES-FEM for accurate analysis of 3D mid-frequency acoustics using tetrahedron mesh,” *Computers & Structures*, vol. 106-107, pp. 125–134, 2012.
- [21] Z. C. He, G. Y. Li, G. R. Liu, A. G. Cheng, and E. Li, “Numerical investigation of ES-FEM with various mass redistribution for acoustic problems,” *Applied Acoustics*, vol. 89, pp. 222–233, 2015.
- [22] L. Y. Yao, D. J. Yu, X. Y. Cui, and X. G. Zang, “Numerical treatment of acoustic problems with the smoothed finite element method,” *Applied Acoustics*, vol. 71, no. 8, pp. 743–753, 2010.
- [23] L. Y. Yao, D. J. Yu, and J. W. Zhou, “Numerical treatment of 2D acoustic problems with the cell-based smoothed radial point interpolation method,” *Applied Acoustics*, vol. 73, no. 6-7, pp. 557–574, 2012.
- [24] T. T. Nguyen, G. R. Liu, K. Y. Lam, and G. Y. Zhang, “A face-based smoothed finite element method (FS-FEM) for 3D linear and nonlinear solid mechanics problems using 4-node tetrahedral elements,” *International Journal for Numerical Methods in Engineering*, vol. 78, pp. 324–353, 2009.
- [25] Z. C. He, G. R. Liu, Z. H. Zhong, X. Y. Cui, G. Y. Zhang, and A. G. Cheng, “A coupled edge-/face-based smoothed finite element method for structural-acoustic problems,” *Applied Acoustics*, vol. 71, no. 10, pp. 955–964, 2010.
- [26] G. Wang, X. Y. Cui, Z. M. Liang, and G. Y. Li, “A coupled smoothed finite element method (S-FEM) for structural-acoustic analysis of shells,” *Engineering Analysis with Boundary Elements*, vol. 61, pp. 207–217, 2015.
- [27] G. R. Liu, T. T. Nguyen, and K. Y. Lam, “A novel alpha finite element method (α FEM) for exact solution to mechanics problems using triangular and tetrahedral elements,” *Computer Methods in Applied Mechanics and Engineering*, vol. 197, no. 45–48, pp. 3883–3897, 2008.
- [28] Z. C. He, G. R. Liu, Z. H. Zhong, G. Y. Zhang, and A. G. Cheng, “Dispersion free analysis of acoustic problems using the alpha finite element method,” *Computational Mechanics*, vol. 46, no. 6, pp. 867–881, 2010.
- [29] Z.-Q. Zhang and G. R. Liu, “Solution bound and nearly exact solution to nonlinear solid mechanics problems based on the smoothed FEM concept,” *Engineering Analysis with Boundary Elements*, vol. 42, pp. 99–114, 2014.
- [30] E. Li, Z. C. He, X. Xu, and G. R. Liu, “Hybrid smoothed finite element method for acoustic problems,” *Computer Methods in Applied Mechanics and Engineering*, vol. 283, pp. 664–688, 2015.
- [31] W. Zeng, G. R. Liu, D. Li, and X. W. Dong, “A smoothing technique based beta finite element method (β FEM) for crystal plasticity modeling,” *Computers & Structures*, vol. 162, pp. 48–67, 2016.
- [32] W. Zeng, G. R. Liu, C. Jiang, T. Nguyen-Thoi, and Y. Jiang, “A generalized beta finite element method with coupled smoothing techniques for solid mechanics,” *Engineering Analysis with Boundary Elements*, vol. 73, pp. 103–119, 2016.
- [33] G. R. Liu, “On G space theory,” *International Journal of Computational Methods*, vol. 6, no. 2, pp. 257–289, 2009.
- [34] G. R. Liu, “A weakened weak (W2) form for a unified formulation of compatible and incompatible methods, part I: theory and part II: applications to solid mechanics problems,” *International Journal for Numerical Methods in Engineering*, vol. 81, pp. 1093–1156, 2010.



Hindawi

Submit your manuscripts at
www.hindawi.com

